CrystEngComm

COMMUNICATION

View Article Online
View Journal | View Issue

Cite this: *CrystEngComm*, 2022, **24**, 479

Received 26th October 2021,
Accepted 30th November 2021

DOI: 10.1039/d1ce01449h

rsc.li/crystengcomm

Efficient degradation of reactive brilliant red on the first open-framework borate-rich cadmium borophosphate†

Yuquan Feng, * Linxia Lv, Dongqin Bi, Zhiguo Zhong, Jing Li, Zilong Yue, Zhaoge Zeng, Shuhan Zhang and Zhaohui Meng

A novel open-framework borate-rich cadmium borophosphate has been obtained by the boric acid reflux method. The compound exhibits a complicated network which is composed of CdO_6 octahedra and an interesting 1D wheel-shaped anion, $_\infty\{[BO_2(OH)]_3B_6P_6O_{27}\}^{12n-}$, built from trigonal-planar $BO_2(OH)$, tetrahedral BO_4 and PO_4 units. This work not only features the first open-framework borate-rich (B/P > 1) cadmium borophosphate, but also exhibits its excellent ion-exchange capacities with Na^+ cations and efficient photocatalytic activities for the degradation of reactive brilliant red (X3B).

Metal borophosphates have shown wide application prospects during the last few years in the fields of ion exchange, adsorption, catalysis and second-order nonlinear optics.[1] Driven by their attractive properties, materials scientists are committed to the synthesis and exploration of metal borophosphates with fascinating structural features. Various synthesis methods, such as hydrothermal, solvothermal, ionothermal and high-temperature solid-phase synthesis methods, have been widely used in the design of metal borophosphates.[2] This results in a large number of borophosphates with different B/P ratios and various FBUs being reported. The structures of borophosphates have also developed from oligomeric units, chains/ribbons, and layered structures to 3D open-framework structures.[3] So far, borophosphates containing alkali metal cations (Li^+–Cs^+), alkali-earth metal cations (Mg^{2+}–Ba^{2+}) and the first transition system metal cations (Sc^{3+}–Zn^{2+}) have been discovered and reported.[4] However, among these known borophosphates, most of them exhibit a lower dimensional structure, and their B/P ratios are usually less than or equal to 1.0; there are only a few borophosphates possessing a 3D open-framework, and their B/P ratios are larger than 1.0.[5,6] Moreover, very few efforts have been made to enrich the family of borate-rich open-framework borophosphates with B/P > 1 by combining Cd^{2+} polyhedra, $B\Phi_3$, $B\Phi_4$ and $P\Phi_4$ (Φ = O/OH) groups. To date, only one example of open-framework Cd^{2+} borophosphate $Na_3Cd_3B(PO_4)_4$ with B/P = 1/4 (B/P < 1) has been reported.[1b] To the best of our knowledge, open-framework Cd^{2+} borophosphate with B/P > 1 has never been discovered in the whole family of borophosphates. As we know, trigonal-planar $\{BO_2(OH)\}$ groups are generally observed in borate-rich borophosphates with B/P > 1.[5] When the $B\Phi_3$, $B\Phi_4$ and $P\Phi_4$ (Φ = O/OH) groups coexist in a single complex, this can easily lead to the formation of chiral or asymmetric molecular structures and endow materials with new condensation patterns and excellent second-order NLO properties.[6] Also, colourless Cd^{2+} cations can exhibit flexible coordination behavior (CdO_6 and CdO_7), which is very conducive to the generation of new structural features and wide transmission range in the UV-visible region.[7a] In addition, Cd^{2+}-containing complexes always exhibit structural diversities and interesting luminescence properties.[7b] Based on the above considerations, we plan to carry out the design and synthesis of 3D open-framework cadmium borophosphates with B/P > 1. As part of our ongoing research,[7a,8] herein, we have successfully synthesized a novel 3D open-framework borophosphate, $[Na(H_2O)][K(H_2O)]\{Na_4Cd_3[BO_2(OH)]_3B_6P_6O_{27}\}$ (B/P = 3/2) (**1**), by means of the boric acid reflux method. This work not only features the first borate-rich (B/P > 1) open-framework cadmium borophosphate, but also exhibits its efficient photocatalytic activities for the degradation of reactive brilliant red (X3B). To the best of our knowledge, it is the first investigation where metal borophosphate was used as the catalyst for photocatalytic degradation in the series of borophosphates.

X-ray structural analysis indicated that **1** crystallizes in the centrosymmetric hexagonal crystal system with the space

College of Chemistry and Pharmacy Engineering, Nanyang Normal University, Nanyang 473061, China. E-mail: yqfeng2008@126.com; Fax: +86 377 6351 3583; Tel: +86 377 6351 3583

† Electronic supplementary information (ESI) available: Supporting figures: the FBU of the borophosphate anion, EDS, PXRD for **1**, IR, luminescence curve, CIE (1931) chromaticity diagram, TG curve, BVS and the selected bond lengths and angles (CCDC: 2112879). For ESI and crystallographic data in CIF or other electronic format see DOI: 10.1039/d1ce01449h

group $P6_3/m$ (no. 176), and its whole structure can be regarded as a 3D open-framework built by alternating linkage of CdO_6 octahedra, BO_4, $\{BO_2(OH)\}$ and PO_4 group units *via* shared corners. The asymmetric structural unit of **1** consists of one independent Cd site, two B sites, one P site, six O sites, one –OH group and two water molecules, as well as one K site and two Na sites acting as counteracting cations. Fig. 1 shows the coordination environment of the Cd(1), B(1), B(2) and P(1) sites. The Cd^{2+} cation is six-coordinated by six O atoms to generate a slightly distorted octahedron with Cd–O bond distances ranging from 2.222(10) to 2.370(9) Å.[1b,7] The B(1) and B(2) atoms exhibit two different coordination modes: the B(1) atom is tetrahedrally coordinated by four oxygen atoms [O(1), O(2), O(3) and O(6)], while the B(2) atom is triangularly coordinated by two oxygen atoms [O(6) and $O(6)^i$; $i = x, y, 1/2 - z$] and one –O(7)H group resulting in a trigonal-planar $\{BO_2(OH)\}$ unit. The P(1) atom adopts four O atoms [O(2), O(3), O(4) and O(5)] leading to a tetrahedral geometric configuration. The B–O bond lengths range from 1.346(14) to 1.507(17) Å, and the P–O bond distances lie between 1.503(9) and 1.552(9) Å.[3] The abovementioned Cd–O, B–O and P–O bond lengths are all in their expected ranges and comparable with those observed in known borophosphates.[4] The results of bond valence calculations[9] revealed that the oxidation states of cadmium, boron and phosphorus sites are in their normal valence +II, +III and +V, respectively. The O(7) sites are protonated hydroxyl groups (–OH groups), while the other O atoms are in their normal oxidation state –II.

Two BO_4 units and one $\{BO_2(OH)\}$ unit are connected by sharing oxygen atoms to yield a $\{B_3O_7(OH)\}$ trimer, and the $\{B_3O_7(OH)\}$ trimer is linked with the surrounding two PO_4 groups, resulting in a cluster $\{B_3P_2O_{11}(OH)\}$ which can be regarded as the FBU of the borophosphate anion (Fig. S1†). These adjacent FBUs are further extended *via* O atoms from the PO_4 groups into a 1D wheel-shaped borophosphate anion, $_\infty\{[BO_2(OH)]_3B_6P_6O_{27}\}^{12n-}$ (Fig. 2). The 1D wheel-shaped borophosphate anion contains $\{B_6P_6\}$ 12-MRs which are

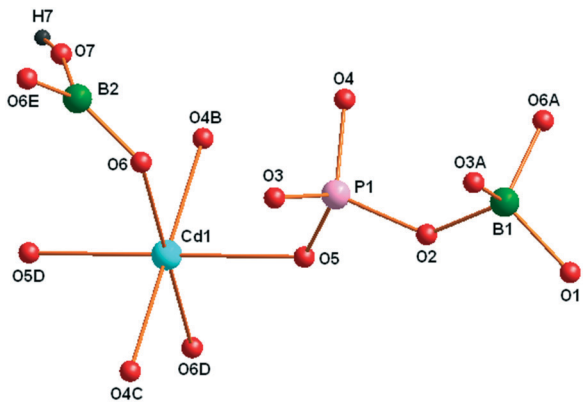

Fig. 1 The coordination environment for the Cd(1), B(1), B(2) and P(1) sites. Symmetry codes: A: $x - y, -1 + x, 1 - z$; B: $1 - y, x - y, z$; C: $1 + y, 1 - x + y, 1 - z$; D: $2 - x, 1 - y, 1 - z$; E: $x, y, 1/2 - z$. Colour codes: Cd(1): turquoise; B(1) and B(2): green; P(1): rose; O atoms: red.

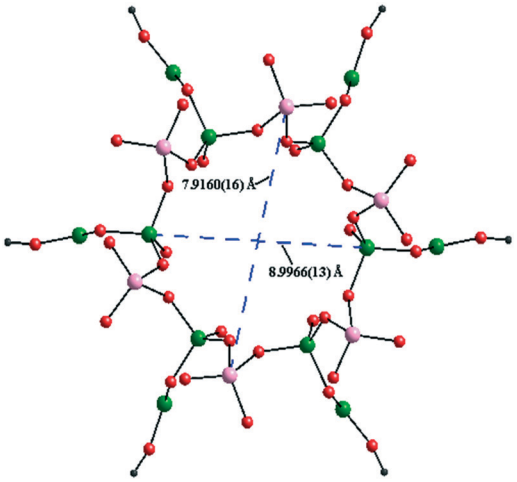

Fig. 2 View of the wheel-shaped borophosphate anion $_\infty\{[BO_2(OH)]_3B_6P_6O_{27}\}^{12n-}$ containing $\{B_6P_6\}$ 12-MR along the *c*-axis. Colour codes: B(1) and B(2): green; P(1): rose; O atoms: red.

constructed by the alternating linkage of six BO_4 groups and six PO_4 groups. The size of $\{B_6P_6\}$ 12-MR is 7.9160(16) Å × 8.9966(13) Å. Within the borophosphate anion $_\infty\{[BO_2(OH)]_3B_6P_6O_{27}\}^{12n-}$, $\{B_6P_4\}$ 10-MR (9.6307(17) Å × 5.7595(9) Å) that is constructed from six BO_4 groups from four different $\{B_3O_7(OH)\}$ trimers and four PO_4 groups can be observed along the *a*-axis (Fig. 3). In other words, each PO_4 group is connected to two neighboring $\{B_3O_7(OH)\}$ trimers, while each $\{B_3O_7(OH)\}$ trimer is surrounded by four adjacent PO_4 groups. Then the borophosphate anion $_\infty\{[BO_2(OH)]_3B_6P_6O_{27}\}^{12n-}$ is further connected with the Cd^{2+} cations by bridging O atoms, forming a 3D open-framework structure (Fig. 4). In the open-framework, each Cd^{2+} cation is bonded to two adjacent borophosphate anions, and each borophosphate anion is linked to six Cd^{2+} cations. In order to better study the connection modes of the open-framework structure, a topological approach[10] was applied to simplify such a 3D architecture. If each $\{B_3O_7(OH)\}$ trimer was viewed as a single node, the 3D structure could be simplified as a 6-, 6- and 4-connected topological network. The topological structure for the open-framework along the *c*-axis is shown in Fig. 5.

The EDS experimental analysis shows that **1** consists of the Cd, K, Na, P, B and O elements (Fig. S2†). The result is in good agreement with that of X-ray structural analysis. In order to confirm the purity of the as-synthesized products,

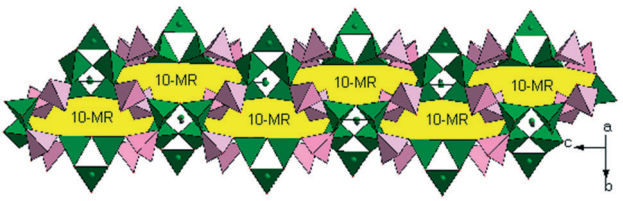

Fig. 3 View of the 1D borophosphate anionic chain exhibiting $\{B_6P_4\}$ 10-MR along the *a*-axis. Colour codes: $BO_2(OH)$ and BO_4: green; PO_4: rose; 10-MR: yellow.

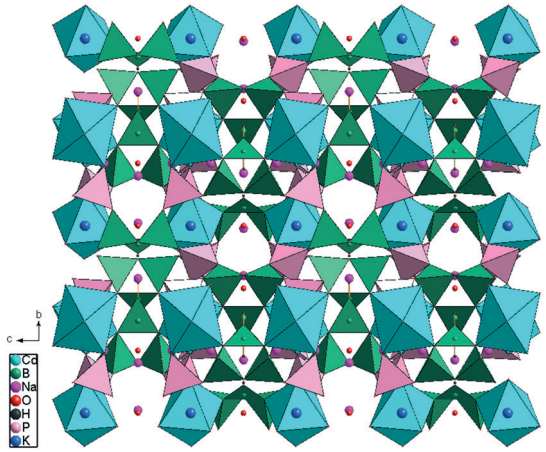

Fig. 4 The 3D open-framework structure of **1**.

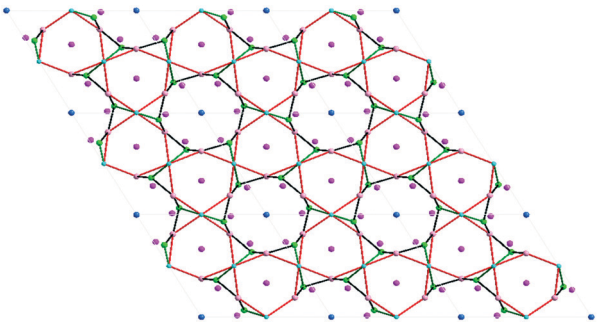

Fig. 5 View of the topological structure for the open-framework along the *c*-axis. Colour codes: {$B_3O_7(OH)$} nodes: bright green; P nodes: rose; Cd nodes: turquoise; Na nodes: pink; K nodes: light blue.

the powder XRD pattern of **1** was obtained. The results revealed that the experimental powder XRD pattern is in agreement with the simulated pattern of the single-crystal structure (Fig. S3†). In addition, the IR spectrum of **1** was studied between 400 and 4000 cm^{-1} (KBr pellet) (Fig. S4†). The peaks at 3455 and 1641 cm^{-1} can be assigned to the stretching and bending vibrations of the –OH units (water molecules and $BO_2(OH)$ groups). The peaks at 1403 and 1267 cm^{-1} can be ascribed to the stretching and bending vibrations of the BO_3 groups. The peaks at 1013, 852 and 614 cm^{-1} are attributed to the symmetric stretching and bending vibrations of the BO_4 groups, respectively. The peaks at 1115 and 928 cm^{-1} and 810, 674, 560 and 555 cm^{-1} are attributed to the asymmetric stretching and bending vibrations of the P–O bonds, respectively.[8a,e] Furthermore, the peaks at 470 and 419 cm^{-1} can be assigned to the K–O and Na–O bonds.

The UV-vis diffuse-reflectance spectrum of **1** was obtained on a UH4150 spectrophotometer. According to the absorbance data between 200–800 nm, an $(ahv)^2$ *versus* optical energy (hv) curve was generated by means of the Tauc plot method and is shown in Fig. 6. The optical band gap of 3.79 eV of **1** (UV absorption cutoff edge: 327 nm) is comparable to that of the borophosphate compound $Na_3Cd_3B(PO_4)_4$ (3.44 eV and 360 nm).[1b] Moreover, the luminescence

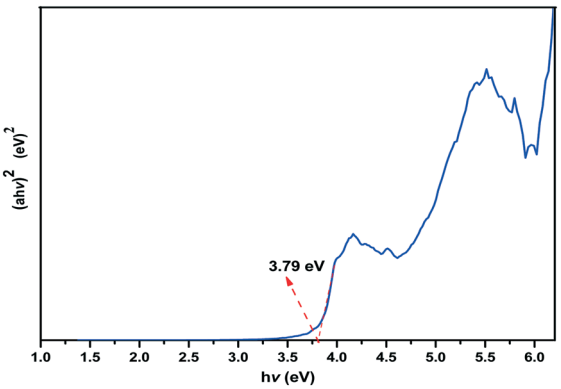

Fig. 6 UV-vis diffuse reflectance spectrum for **1**.

properties of **1** in the solid-state were also studied at RT (Fig. S5†). Upon excitation at 225 nm, strong emission occurs with the maximum at 342 nm. The emission may be ascribed to the {$BO_2(OH)$}, BO_4 and PO_4 groups in the borophosphate anion $_\infty\{[BO_2(OH)]_3B_6P_6O_{27}\}^{12n-}$. The results of the luminescence test are also in agreement with those of UV-vis diffuse-reflectance. The CIE chromaticity coordinate (x, y) is calculated according to the emission peak. Fig. S6† shows the CIE (1931) chromaticity diagram of **1**. The x and y values are 0.234 and 0.226, respectively, which are located in the blue region. In addition, the lifetime of **1** (Fig. 7) has also been studied (λ_{ex} = 225 nm and λ_{em} = 342 nm). The plot of counts *versus* time could be well fitted according to the double-exponential equation [$I = A_1\exp(-t/\tau_1) + A_2\exp(-t/\tau_2)$] with a calculated τ value of 1.74 ns.

The ion-exchange capacities of **1** with Na^+ cations have been studied. The crystalline sample of **1** (0.014 g) and 0.1 mmol Na^+ ions (0.179 g $Na_2HPO_4{\cdot}12H_2O$/5.84 mg NaCl/8.50 mg $NaNO_3$/13.6 mg $CH_3COONa{\cdot}3H_2O$) were placed in a Teflon-lined stainless-steel autoclave (50 mL) at 220 °C for 12 hours.[11] The ion-exchanged crystals were repeatedly washed with deionized water and detected by EDS (Fig. S7†), ICP-MS and PXRD (Fig. S3†), and the experimental result reveals that the K^+ cations in **1** can be completely exchanged with the Na^+

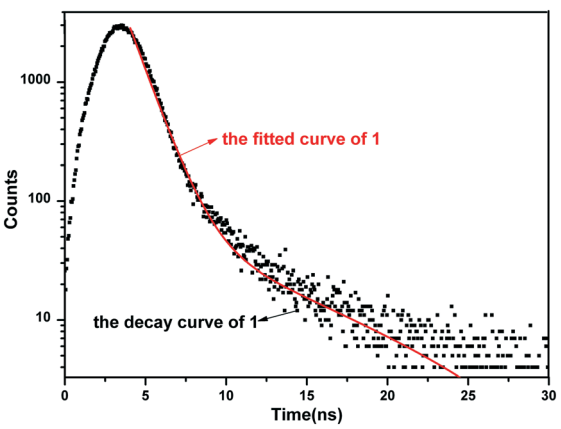

Fig. 7 The decay curves for **1** in the solid-state at room temperature.

cations and the structure can remain stable after the ion-exchange experiment.

The thermal stability of **1** was studied in the range of 30–900 °C with a heating rate of 10 °C min^{-1} in a dynamic N_2 atmosphere (gas flow: 0.1 L min^{-1}). The experimental results indicate a total mass loss of 4.55% between 81 and 769 °C in two steps ($\Delta m_{calcd}/m$ = 4.52%) (Fig. S8†). In the first step, between 81 and 437 °C, the weight is reduced by 1.24%, which corresponds to the release of one water molecule ($\Delta m_{calcd}/m$ = 1.27%). In the second step, between 437 and 769 °C, the weight decreases by 3.31%, which is attributed to the loss of one water molecule and three –OH groups (2.5 water molecules, $\Delta m_{calcd}/m$ = 3.25%).[8e] The loss of three –OH groups was observed in the second step, indicating that the decomposition of the open-framework should occur in this stage. In order to better confirm the composition of the final product after thermal analysis, EDS experimental analysis was performed. The results reveal that the final product may be metallic oxide containing Na, K, Cd, P, B and O elements.

Considering the fact that colourless borophosphate probably exhibits photocatalytic activities, we are interested in investigating its photocatalytic properties for the degradation of organic complexes. The catalyst photoactivity was evaluated by using X3B (the reactive brilliant red) degradation in water as a model reaction. The UV light source was a high-pressure mercury lamp (375 W) equipped with Pyrex glass. The experiment was carried out in a thermostated reactor under fixed conditions (1.00 g L^{-1} catalyst, 40 ppm X3B, and 10 mM H_2O_2). At the given intervals of light irradiation, small aliquots were taken and filtered through a membrane (0.22 μm). The X3B concentration in solution was analyzed by measuring its maximal absorbance at 511 nm using a V2200 spectrometer.

Due to the fact that reactive brilliant red (X3B) is hardly adsorbed on catalyst **1**, all the suspensions containing the necessary components were first sonicated for 5 min and shaken in the dark for 30 min to achieve equilibrium before light irradiation. Fig. 8 shows the curve for the degradation of X3B under different conditions in aqueous solution. The results reveal that X3B itself degrades slightly under UV light (curve b), which is due to the fact that the dye itself can absorb light and undergo photolysis. In aqueous solution, the photodegradation of organic complexes is very slow due to the inability to reduce O_2 by the conduction electrons on the irradiated catalyst (curve c). The organic complexes degrade more rapidly when H_2O_2 is present (curve d), which is in good agreement with the fact that H_2O_2 is a better electron acceptor than O_2. It can capture the conduction electrons of the catalyst and produce an active species, $^{\cdot}OH$, which can mineralize most organic pollutants.[12] The control experiments show that the organics were not degraded or degraded very slowly in the absence of light or in the absence of a catalyst (curves a and d), respectively. This indicates that the Fenton-like reaction between H_2O_2 and the catalyst is not efficient, and it is very difficult to photolyze H_2O_2 directly under the present conditions. In the presence of both the catalyst and H_2O_2, the degradation of organics under light is very obvious (curve e).

For practical use in water treatments, the catalyst stability is also an important factor to be considered. For this concern, recycling experiments were performed for X3B degradation under UV light irradiation under the same conditions as described above. After each run was completed, 6.0 mL of stock solution with X3B (40 ppm) and H_2O_2 (10 mM) was supplied to restore the initial concentration, and then the same steps were repeated. The catalyst activity was still excellent even after six runs (Fig. 9), and the reaction rate just slightly decreased from one run to another. Such a decrease in the reaction rate may be attributed to the gradually decreased catalyst concentration and the effection of intermediates. The result shows that the catalyst has a high stability during the recycling experiments, and **1** can act as an efficient catalyst for the degradation of reactive brilliant red (X3B).

In summary, a novel 3D open-framework borate-rich cadmium borophosphates with B/P > 1 was prepared through the boric acid flux method. The UV-vis diffuse-reflectance spectrum reveals an optical band gap of 3.79 eV and a UV

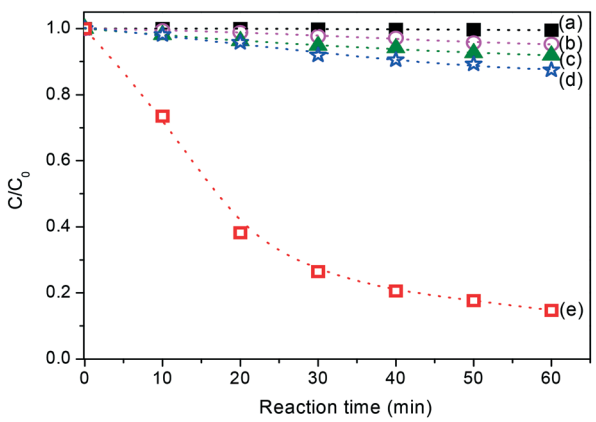

Fig. 8 Time profiles of X3B degradation under different conditions: (a) **1** + H_2O_2 + dark; (b) O_2 + UV; (c) **1** + O_2 + UV; (d) H_2O_2 + UV; (e) **1** + H_2O_2 + UV.

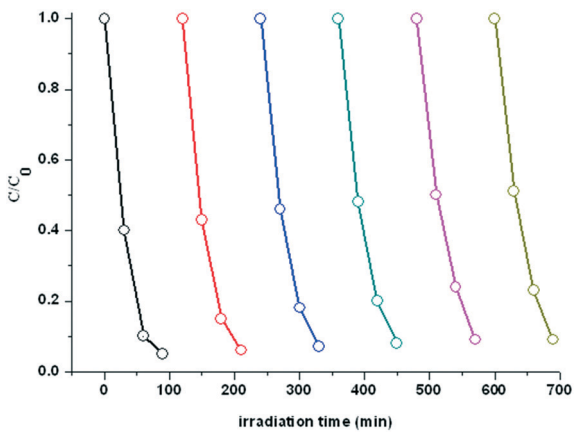

Fig. 9 Recycling experiment for X3B degradation under UV light in the presence of H_2O_2 over **1** in aqueous solution.

absorption cutoff edge at 327 nm. **1** shows a strong emission peak at 342 nm with a lifetime of 1.74 ns upon excitation at 225 nm. The ion-exchange experiment reveals that the K^+ cations in **1** can be completely exchanged with the Na^+ cations in a Teflon-lined stainless-steel autoclave (50 mL) at 220 °C for 12 hours. Moreover, **1** exhibits efficient photocatalytic activities for the degradation of reactive brilliant red (X3B). This is the first example of the use of metal borophosphate as the catalyst for photocatalytic degradation in the series of borophosphates. This work indicates that **1** can act as a new potential photocatalytic material. The successful synthesis of **1** predicts that more open-framework cadmium borophosphates with attractive structural features and applications would be prepared in the near future.

Author contributions

Yuquan Feng: first author and corresponding author, conceptualization, methodology, and writing – original draft; Linxia Lv: writing – reviewing and editing; Dongqin Bi: sample preparation; Zhiguo Zhong: data collection and structure refinement; Jing Li, Zilong Yue and Zhaoge Zeng: property test; Shuhan Zhang: sample characterization; Zhaohui Meng: validation.

Conflicts of interest

There are no conflicts of interest to declare.

Acknowledgements

This work was financially supported by the National Natural Science Foundation of China (no. 21601095) and the Youth Project of Nanyang Normal University (no. QN208259, 2022QN002).

Notes and references

1 (*a*) Z. Y. Bai, L. H. Liu, L. Z. Zhang, Y. S. Huang, F. F. Yuan and Z. B. Lin, *Chem. Commun.*, 2019, **55**, 8454; (*b*) Y. J. Shi, S. L. Pan, X. Y. Dong, Y. Wang, M. Zhang, F. F. Zhang and Z. X. Zhou, *Inorg. Chem.*, 2012, **51**, 10870; (*c*) P. A. Maggard, C. L. Stern and K. R. Poeppelmeier, *J. Am. Chem. Soc.*, 2011, **123**, 7742; (*d*) X. L. Chen, B. B. Zhang, F. F. Zhang, Y. Wang, M. Zhang, Z. H. Yang, K. R. Poeppelmeier and S. L. Pan, *J. Am. Chem. Soc.*, 2018, **140**, 16311; (*e*) H. P. Wu, H. W. Yu, Z. H. Yang, X. L. Hou, S. L. Pan, X. Su, K. R. Poeppelmeier and J. M. Rondinelli, *J. Am. Chem. Soc.*, 2013, **135**, 4215; (*f*) X. Y. Dong, Q. Jing, Y. J. Shi, Z. H. Yang, S. L. Pan, K. R. Poeppelmeier, J. Young and J. M. Rondinelli, *J. Am. Chem. Soc.*, 2015, **137**, 9417; (*g*) M.-R. Li, W. Liu, M.-H. Ge, H.-H. Chen, X.-X. Yang and J.-T. Zhao, *Chem. Commun.*, 2004, 1272; (*h*) P. Liang and Z.-H. Liu, *CrystEngComm*, 2016, **18**, 1311; (*i*) Y. Wang, S. L. Pan, S. J. Han, B. B. Zhang, L. Y. Dong, M. Zhang and Z. H. Yang, *CrystEngComm*, 2014, **16**, 6848.

2 (*a*) Y. Wang, B. B. Zhang, Z. H. Yang and S. L. Pan, *Angew. Chem., Int. Ed.*, 2018, **57**, 2150; (*b*) H. P. Wu, S. L. Pan, K. R. Poeppelmeier, H. Y. Li, D. Z. Jia, Z. H. Chen, X. Y. Fan, Y. Yang, J. M. Rondinelli and H. Luo, *J. Am. Chem. Soc.*, 2011, **133**, 7786; (*c*) F. Kong, S.-P. Huang, Z.-M. Sun, J.-G. Mao and W.-D. Cheng, *J. Am. Chem. Soc.*, 2006, **128**, 7750; (*d*) S. L. Pan, J. P. Smit, B. Watkins, M. R. Marvel, C. L. Stern and K. R. Poeppelmeier, *J. Am. Chem. Soc.*, 2006, **128**, 11631; (*e*) L. Wang, S. L. Pan, L. X. Chang, J. Y. Hu and H. W. Yu, *Inorg. Chem.*, 2012, **51**, 1852; (*f*) X. Fan, S. L. Pan, J. Guo, X. Hou, J. Han, F. Zhang, F. Li and K. R. Poeppelmeier, *J. Mater. Chem.*, 2013, **1**, 10389.

3 (*a*) Y. J. Shi, S. L. Pan, X. Y. Dong, Y. Wang, M. Zhang, F. F. Zhang and Z. X. Zhou, *Inorg. Chem.*, 2012, **51**, 10870; (*b*) W.-L. Zhang, W.-D. Cheng, H. Zhang, L. Geng, C.-S. Lin and Z.-Z. He, *J. Am. Chem. Soc.*, 2010, **132**, 1508; (*c*) H. S. Ra, K. M. Ok and P. S. Halasyamani, *J. Am. Chem. Soc.*, 2003, **125**, 7764; (*d*) X. Xu, C.-L. Hu, F. Kong, J.-H. Zhang, J.-G. Mao and J. L. Sun, *Inorg. Chem.*, 2013, **52**, 5831; (*e*) B. B. Zhang, G. G. Shi, Z. H. Yang, F. F. Zhang and S. L. Pan, *Angew. Chem., Int. Ed.*, 2017, **56**, 3916.

4 (*a*) X. F. Wang, Y. Wang, B. B. Zhang, F. F. Zhang, Z. H. Yang and S. L. Pan, *Angew. Chem., Int. Ed.*, 2017, **56**, 14119; (*b*) G. Q. Shi, Y. Wang, F. F. Zhang, B. B. Zhang, Z. H. Yang, X. L. Hou, S. L. Pan and K. R. Poeppelmeier, *J. Am. Chem. Soc.*, 2017, **139**, 10645; (*c*) M. D. Mutailipu, M. Zhang, B. B. Zhang, L. L. Wang, Z. H. Yang, X. Zhou and S. L. Pan, *Angew. Chem., Int. Ed.*, 2018, **57**, 6095; (*d*) D. Zhao, W.-D. Cheng, H. Zhang, S.-P. Huang, Z. Xie, W.-L. Zhang and S.-L. Yang, *Inorg. Chem.*, 2009, **48**, 6623; (*e*) K. M. Ok and P. S. Halasyamani, *Inorg. Chem.*, 2005, **44**, 3919.

5 M. Li and A.-V. Mudring, *Cryst. Growth Des.*, 2016, **16**, 2441.

6 R. Kniep, H. Engelhardt and C. Hauf, *Chem. Mater.*, 1998, **10**, 2930.

7 (*a*) Y. Q. Feng, H. T. Fan, Z. G. Zhong, H. W. Wang and D. F. Qiu, *Inorg. Chem.*, 2016, **55**, 11987; (*b*) X. Feng, J. Liu, J. Li, L. F. Ma, L. Y. Wang, S. W. Ng and G. Z. Qin, *J. Solid State Chem.*, 2015, **230**, 80.

8 (*a*) Y. Q. Feng, Z. K. Li, Z. G. Zhong, H. W. Wang and D. F. Qiu, *Dalton Trans.*, 2020, **49**, 1388; (*b*) Y. Q. Feng, M. Li, H. T. Fan, Q. Z. Huang, D. F. Qiu and H. Z. Shi, *Dalton Trans.*, 2015, **44**, 894; (*c*) Y. Q. Feng, D. F. Qiu, H. T. Fan, M. Li, Q. Z. Huang and H. Z. Shi, *Dalton Trans.*, 2015, **44**, 8792; (*d*) Y. Q. Feng, C. H. Ding, H. T. Fan, Z. G. Zhong, D. F. Qiu and H. Z. Shi, *Dalton Trans.*, 2015, **44**, 18731; (*e*) Y. Q. Feng, M. Li, H. Z. Shi, Q. Z. Huang and D. F. Qiu, *CrystEngComm*, 2013, **15**, 2048; (*f*) Y. Q. Feng, Z. G. Zhong, H. W. Wang, H. T. Fan, D. Q. Bi, L. Wang, Z. Z. Xing and D. F. Qiu, *Chem. – Eur. J.*, 2017, **23**, 9962; (*g*) H. Z. Shi, Y. Q. Feng, Q. Z. Huang, D. F. Qiu, M. Li and K. C. Liu, *CrystEngComm*, 2011, **13**, 7185.

9 I. D. Brown and D. Altermatt, *Acta Crystallogr., Sect. B: Struct. Sci.*, 1985, **41**, 244.

10 X.-J. Ke, D.-S. Li and M. Du, *Inorg. Chem. Commun.*, 2011, **14**, 788.

11 W. T. Yang, J. Y. Li, Q. H. Pan, Z. Jin, J. H. Yu and R. R. Xu, *Chem. Mater.*, 2008, **20**, 4900.

12 (*a*) D. Q. Bi and Y. M. Xu, *Langmuir*, 2011, **27**, 9359; (*b*) D. Q. Bi and Y. M. Xu, *J. Mol. Catal. A: Chem.*, 2013, **367**, 103; (*c*) J. Kim, C. W. Lee and W. Choi, *Environ. Sci. Technol.*, 2010, **44**, 6849; (*d*) R. Abe, H. Takami, N. Murakami and B. Ohtani, *J. Am. Chem. Soc.*, 2008, **130**, 7780.